Internal climate variability modulates decadal changes in ocean anthropogenic carbon storage

Author(s):
Olivarez, Holly C.; Lovenduski, Nicole S.; Maroon, Elizabeth; Müller, Jens D.; Fay, Amanda R.; Krumhardt, Kristen M.; Levy, Michael N.; Lindsay, Keith; McKinley, Galen A.; Rader, Jamin K.

Publication date:
2025-01

Permanent link:
https://doi.org/https://doi.org/10.3929/ethz-b-000716283

Originally published in:
Environmental Research Letters 20(1), https://doi.org/10.1088/1748-9326/ada2ad

ENVIRONMENTAL RESEARCH
LETTERS

CrossMark

OPEN ACCESS

RECEIVED
14 August 2024

REVISED
12 November 2024

ACCEPTED FOR PUBLICATION
23 December 2024

PUBLISHED
9 January 2025

LETTER

Internal climate variability modulates decadal changes in ocean anthropogenic carbon storage

Holly C Olivarez[1,2,*], Nicole S Lovenduski[2,3], Elizabeth Maroon[4], Jens D Müller[5], Amanda R Fay[6], Kristen M Krumhardt[7], Michael N Levy[7], Keith Lindsay[7], Galen A McKinley[6] and Jamin K Rader[8]

[1] Department of Environmental Studies, University of Colorado, Boulder, CO, United States of America
[2] Institute of Arctic and Alpine Research, University of Colorado, Boulder, CO, United States of America
[3] Department of Atmospheric and Oceanic Sciences, University of Colorado, Boulder, CO, United States of America
[4] Department of Atmospheric and Oceanic Sciences, University of Wisconsin-Madison, Madison, WI, United States of America
[5] Environmental Physics, Institute of Biogeochemistry and Pollutant Dynamics, ETH Zürich, Zürich, Switzerland
[6] Columbia University and Lamont-Doherty Earth Observatory, Palisades, NY, United States of America
[7] Climate and Global Dynamics Laboratory, NSF National Center for Atmospheric Research, Boulder, CO, United States of America
[8] Department of Atmospheric Science, Colorado State University, Fort Collins, CO, United States of America
[*] Author to whom any correspondence should be addressed.

E-mail: holly.olivarez@colorado.edu

Keywords: ocean anthropogenic carbon storage, ocean biogeochemistry, CESM2 large ensemble, marine carbon cycle, ocean modeling, internal climate variability, Earth system modeling

Supplementary material for this article is available online

Abstract

The ocean removes man-made (anthropogenic) carbon from the atmosphere and thereby mitigates climate change. Observations from global hydrographic surveys reveal the spatial and temporal evolution of the ocean inventory of anthropogenic carbon and suggest substantial decadal variability in historical storage rates. Here, we use a 100-member ensemble of an Earth system model to investigate the influence of external forcing and internal climate variability on historical changes in ocean anthropogenic carbon storage over 1994 to 2014. Our findings reveal that the externally forced, decadal changes in storage are largest in the Atlantic (2–4 mmol m^{-3} decade^{-1}) and positive nearly everywhere. Internal climate variability modulates regional ocean anthropogenic carbon storage trends by up to 10 mmol m^{-3} decade^{-1}. The influence of internal climate variability on decadal storage changes is most prominent at depths of ∼300 m and at the edges of the subtropical gyres. Internal variability in anthropogenic carbon in the extratropics has high spectral power on decadal to multi-decadal timescales, indicating that the approximately decadal repetitions of hydrographic surveys may produce storage change estimates that are heavily influenced by internal climate variability.

1. Introduction

Nearly one-third of the historical, anthropogenic emissions of carbon dioxide (CO_2) have been absorbed by the ocean (Khatiwala *et al* 2013), mitigating the rate of climate change. As a result, the global ocean inventory of anthropogenic carbon (C_{ant}) has increased from zero in pre-industrial times to more than 170 Pg C today (Canadell *et al* 2021). C_{ant} is heterogeneously distributed in the ocean interior due to ocean circulation patterns. Once C_{ant} enters the surface ocean through air–sea gas exchange, it is slowly transported to the intermediate and deep ocean along isopycnal surfaces that outcrop in certain geographic locations including the subpolar North Atlantic, mid-latitude Southern Ocean, and the subtropical North Pacific (Sarmiento *et al* 1992, Graven *et al* 2012).

Data collected on repeat hydrographic surveys conducted approximately each decade suggest substantial variability in ocean C_{ant} storage rates over 1994 to 2014 (Müller *et al* 2023). According to observation-based estimates, from 1994 to 2004 the global ocean storage of C_{ant} grew by 29 ± 3 Pg C dec^{-1}, whereas the growth rate slowed to 27 ± 3 Pg

C dec^{-1} from 2004 to 2014, despite atmospheric CO_2 growth rates of 18.6 ppm dec^{-1} and 20.4 ppm dec^{-1} over the same respective decades (Müller *et al* 2023). In other words, while the ocean inventory of C_{ant} grew from 1994 to 2014, the rate of storage increase in the second decade was slower than that of the first. Further, studies find that changes in the rate of C_{ant} storage manifest differently in different regions of the ocean, with a slowdown in the storage rate in the North Atlantic, and a speed-up in the storage rate in the South Atlantic in the second decade relative to the first (Gruber *et al* 2019b, Müller *et al* 2023). Future projections of the coupled carbon-climate system would benefit from a deeper understanding of the drivers of change in ocean C_{ant} storage, yet the causes of these storage rate changes remain unknown.

Due to their decadal repetitions, it is challenging to quantify the relative roles of external forcing and internal climate variability in ocean C_{ant} storage changes from hydrographic observations. Externally forced drivers of changes in ocean C_{ant} storage could be driven by changes in atmospheric CO_2 concentrations, changes in ocean transport, changes in ocean buffer capacity, or volcanic eruptions (Revelle and Suess 1957, McKinley *et al* 2017, 2020, Fay *et al* 2023, Olivarez *et al* 2024). Internal climate variability, defined as drivers of change that are not from external forcings, also has the capacity to affect change in ocean C_{ant} storage rates by altering ocean circulation patterns. For example, the Pacific Decadal Oscillation, a low frequency mode of internal climate variability, impacts the subduction of North Pacific subtropical mode water and its associated biogeochemical properties (Oka *et al* 2015). Historical changes in the rate of ocean C_{ant} storage have likely been influenced by a combination of external forcing and internal climate variability.

This study uses a novel, large ensemble modeling approach to de-convolve the relative roles of external forcing and internal climate variability in the spatiotemporal changes in historical ocean C_{ant} storage. We analyze output from the Community Earth System Model version 2 (CESM2) 100-member Large Ensemble, where the ensemble mean changes are attributable to external forcing, and the ensemble standard deviation is ascribed to internal climate variability. We examine regional and depth-resolved decadal changes in C_{ant} storage and determine the timescales of internal variability in C_{ant}.

2. Methods

Our primary numerical tool used in this study is CESM2, which consists of coupled atmosphere, ocean, sea-ice, land surface, and land/ocean carbon cycle model components (Danabasoglu *et al* 2020). The ocean component of CESM2 is the Parallel Ocean Program version 2 (POP2) with nominal 1° resolution, 60 vertical levels, and parameterized sub-grid scale processes (Danabasoglu *et al* 2012). The ocean biogeochemistry model in CESM2 is the Marine Biogeochemistry Library (MARBL), which represents the lower (planktonic) trophic levels of the marine ecosystem, full carbonate system thermodynamics, air–sea CO_2 exchange, and dynamic nutrient (Fe, Si, N, and P) cycling (Moore *et al* 2004, 2013, Moore and Braucher 2008, Long *et al* 2021). The carbonate chemistry module uses prescribed atmospheric CO_2 concentrations to simultaneously solve the full carbonate system using both contemporary and preindustrial atmospheric CO_2 concentration values, such that C_{ant} can be calculated by taking the difference of these two carbonate systems (Lovenduski *et al* 2007, 2008, Long *et al* 2021).

To quantify the impact of external forcing and internal climate variability on ocean C_{ant} storage changes, we use output from a 100-member ensemble of CESM2, which we refer to as CESM2-LE (Rodgers *et al* 2021). We focus our analysis on output from the historical period (1850–2014), where the external forcing for all ensemble members follows that of the 6th Coupled Model Intercomparison Project (CMIP6, Meinshausen *et al* 2017), with two different sets of forcing fields for historical biomass burning emissions DeRepentigny *et al* (2022), which has a negligible influence on internal variability in ocean C_{ant} storage, but a large influence on other aspects of the Earth system, e.g. Arctic sea ice;. The ensemble is generated using both macro- and micro-initialization to create a unique ensemble standard deviation that includes the impact of the initial AMOC state on climate variability. The macro-initialization starts from four different years that correspond with years of maximum, decreasing, minimum, and increasing AMOC transport, respectively, relative to the preindustrial control simulation. The micro-initialization uses independent restart files at 10 yr intervals over 1001 to 1191 (Rodgers *et al* 2021). In our study, the impact of external forcing on ocean C_{ant} is estimated from the mean across the 100 ensemble members, while the impact of internal climate variability on ocean C_{ant} is estimated as the spread across the 100 ensemble members.

Consistent with other global ocean biogeochemical models from the Global Carbon Budget (GOBMs, specified in Müller *et al* 2023), CESM2-LE estimates are lower than the rate of increase in the ocean C_{ant} inventory from 1994 to 2014 as compared to an observation-based estimate using the extended Multiple Linear Regression eMLR(C^*) approach (figure S1; Müller *et al* 2023). From 1994 to 2004, the surface to seafloor in CESM2-LE accumulates 18.6 ± 0.6 Pg C_{ant} dec^{-1}, while the eMLR(C^*) method accumulates 29 ± 2.5 Pg C_{ant} dec^{-1} and the GOBMs accumulate, on average, 19.5 ± 2.7 Pg C_{ant} dec^{-1}. From 2004 to 2014, the CESM2-LE accumulates 21.4 ± 0.7 Pg C_{ant} dec^{-1}, while eMLR(C^*) accumulates 27 ± 2.5 Pg C_{ant} dec^{-1} and the GOBMs accumulate, on average, 22.8 ± 2.7 Pg C_{ant} dec^{-1}. Thus, CESM2-LE is consistent with other GOBMs in underestimating the growth in the oceanic C_{ant} inventory (Hauck *et al* 2020, Terhaar *et al* 2022, 2024, Müller *et al* 2023).

To examine the role of horizontal resolution in ocean C_{ant} storage changes, we also use output from a newly released, global high resolution (0.1°) ocean-ice hindcast simulation of CESM2 (Krumhardt *et al* 2024), which is forced by the JRA55-do product atmospheric state and runoff dataset over the period 1958 to 2021 (Kobayashi *et al* 2015, Tsujino *et al* 2020).

This study examines the decadal change in ocean C_{ant} storage for the decades spanning January 1994 to December 2003, and January 2004 to December 2013. Following the approach of Müller *et al* (2023), we calculate the change in ocean C_{ant} storage between reference years 1994–2004 as

$$\Delta C_{\mathrm{ant}_{d1}} = 2004_{C_{\mathrm{ant}}} - 1994_{C_{\mathrm{ant}}}, \qquad (1)$$

where d1 represents decade 1. Similarly, the change in ocean C_{ant} storage between reference years 2004–2014 is defined as

$$\Delta C_{\mathrm{ant}_{d2}} = 2014_{C_{\mathrm{ant}}} - 2004_{C_{\mathrm{ant}}}. \qquad (2)$$

The decadal change in ocean C_{ant} storage ($\Delta\Delta C_{ant}$) is defined as

$$\Delta\Delta C_{\mathrm{ant}} = \Delta C_{ant_{d2}} - \Delta C_{ant_{d1}}. \qquad (3)$$

We calculate the ensemble standard deviation of the 100 ensemble members over each decade and for the decadal change in ocean C_{ant} storage. The ensemble spread can be measured by its standard deviation ($\sigma(\Delta\Delta C_{ant})$), as it captures the impact of internal variability on the decadal changes in C_{ant}.

We illustrate the spatial structure of the ocean gyres using the model-derived barotropic streamfunction (BSF). BSF is depth-integrated volume transport and illustrates the position of gyres occurring across the global ocean. Detailed information about how BSF is estimated in POP2 can be found in Smith *et al* (2010).

We perform fast Fourier transform (FFT; e.g. Heideman *et al* 1985) analysis of CESM2-LE ensemble members over 1988–2014 to determine the spectral power of internal variability in C_{ant} on different timescales. Upper ocean integrals (top ∼3000 m) of C_{ant} from each ensemble member are prepared for FFT analysis using the following procedure, outlined in Landschützer *et al* (2019). The ensemble mean is subtracted to remove the externally forced response, any residual seasonality is removed by applying a 12 month running mean, and spectral leakage from low-frequency harmonics is suppressed via linearly detrending the residual C_{ant} anomalies. FFT analysis is conducted in each ensemble member at every ocean grid cell and separately. We then sum the spectral power together into four timescales based loosely on large-scale climate modes: a 1–3 yr period, a 3–7 yr period to match ENSO (Feely *et al* 1999, 2006), a 7–20 yr period for PDO (Mantua *et al* 1997, Zhang *et al* 1997) and AMOC (Buckley and Marshall 2016, Zhang *et al* 2019), and a decade-to-century frequency to capture other low-frequency oscillatory climate behavior. The power spectra of all ensemble members are ensemble averaged and then divided by the total power to calculate the fractional variance of the internal variability in each timescale.

3. Results

The externally forced, decadal change in ocean anthropogenic carbon storage ($\Delta\Delta C_{ant}$) is positive nearly everywhere across the global ocean. Figure 1(a) shows the ensemble mean, upper 3000 m integrated $\Delta\Delta C_{ant}$, estimated by subtracting the ensemble mean ΔC_{ant} over the decade 1994-2004 from the ensemble mean ΔC_{ant} over 2004–2014 (equation (3)). The largest positive decadal changes in C_{ant} storage are found in the North Atlantic ($\Delta\Delta C_{ant}$ = 2-4 mol m^{-2} dec^{-1}) and in the Arctic Ocean ($\Delta\Delta C_{ant}$ > 4 mol m^{-2} dec^{-1}). External forcing drives 1-2 mol m^{-2} dec^{-1} increases in C_{ant} storage in the subtropical latitudes of all ocean basins, and 2-3 mol m^{-2} dec^{-1} increases in C_{ant} storage in the South Atlantic (figure 1(a)). These results suggest that external forcing drives increasing rates of C_{ant} storage throughout the global ocean from one decade to the next, with storage rates increasing fastest in the North Atlantic, Arctic, and subtropical South Atlantic.

Externally forced, decadal changes in ocean C_{ant} storage are heterogeneously distributed with depth (figure 2(a)). The largest changes occur at ∼100 m in the tropics, at ∼300 m in the subtropics, and at ∼500 m in the subpolar North Atlantic and Arctic (figure 2(a)). Externally forced $\Delta\Delta C_{ant}$ is positive across the global ocean at the surface, 100 m, and 500 m, and mostly positive at 300 m, with the exception of the western Pacific warm pool, where $\Delta\Delta C_{ant}$ is a small negative number (figure 2(a)). The mostly positive, externally forced $\Delta\Delta C_{ant}$ values extend to depths of 3000 m and beyond (not shown). The ensemble mean, zonal mean $\Delta\Delta C_{ant}$ confirms that externally forced, decadal C_{ant} storage changes are most prominent in the North Atlantic (2-4 mmol m^{-3} dec^{-1} from 20°N to the Arctic and ∼250 to ∼1000 m depth) (figure 3, upper panel).

Though internal variability has only a small effect on the temporal evolution of the global, cumulative C_{ant} storage inventory (pink shading in figure S1), on regional scales, internal variability in the decadal change in ocean C_{ant} storage is the same order of magnitude as the externally forced decadal change (figure 1). In the subpolar North Atlantic, the ensemble standard deviation of the decadal change

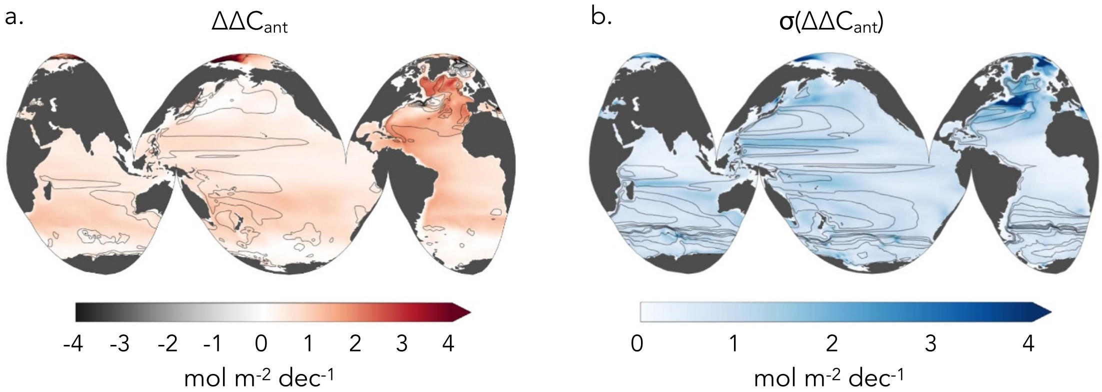

Figure 1. (a) Ensemble mean, decadal change in upper ocean (0–3000 (m) integrated C_{ant} storage from 1994 to 2014 ($\Delta\Delta C_{ant}$; mol m^{-2} dec^{-1}). (b) Ensemble standard deviation of the decadal change in upper ocean integrated C_{ant} storage ($\Delta\Delta C_{ant}$); mol m^{-2} dec^{-1}). Colorbar in (b) is replicated as black contours in (a). Contours in (b) show the ensemble mean barotropic streamfunction (BSF) over 1994–2004. Contours are every 10 Sv with zero-contour omitted.

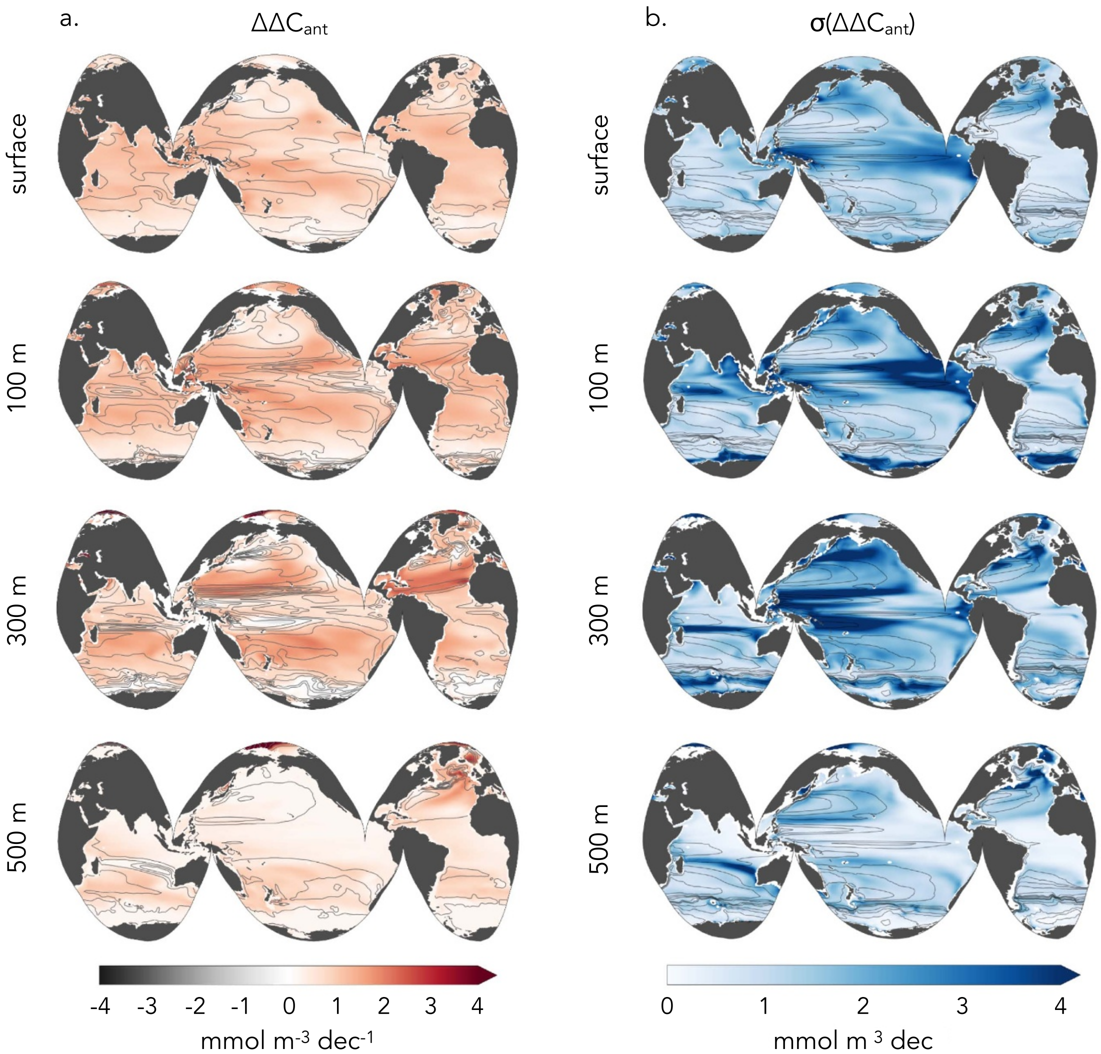

Figure 2. (a) Ensemble mean, decadal change in C_{ant} storage from 1994 to 2014 at the surface, ∼100 m, ∼300 m, and ∼500 m ($\Delta\Delta C_{ant}$; mmol m^{-3} dec^{-1}). (b) Ensemble standard deviation of the decadal change in storage at the same depths ($\sigma(\Delta\Delta C_{ant})$; mmol m^{-3} dec^{-1}). Colorbar in column (b) is replicated as black contours in column (a). Contours in column (b) show the ensemble-mean barotropic streamfunction (BSF) over 1994–2004. Contours are every 10 Sv with zero-contour omitted.

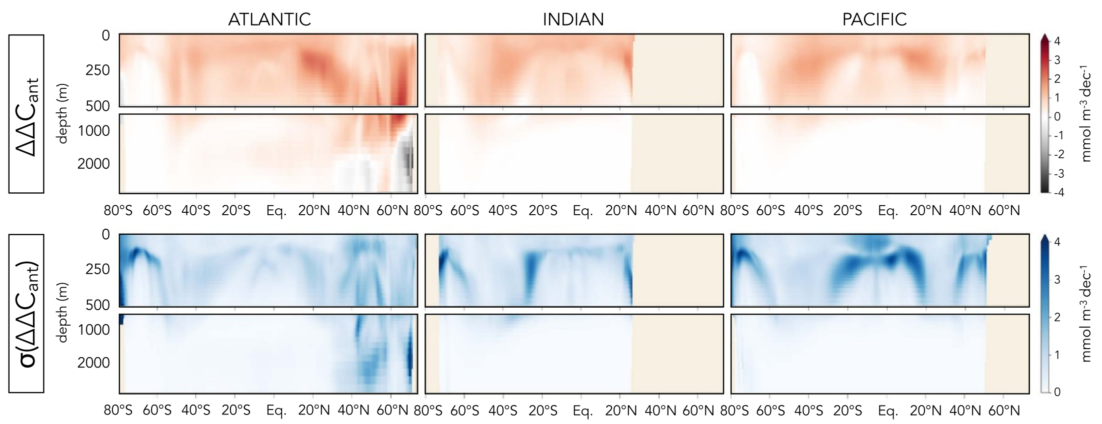

Figure 3. (upper) Ensemble mean, zonal mean decadal change in C_{ant} storage from 1994 to 2014 in the Atlantic, Indian, and Pacific basins from the surface to ~3000 m ($\Delta\Delta C_{ant}$; mmol m^{-3} dec^{-1}). (lower) Ensemble standard deviation of the decadal change in storage in the same basins ($\sigma(\Delta\Delta C_{ant})$; mmol m^{-3} dec^{-1}).

in upper ocean (0–3000 m) integrated C_{ant} storage ($\sigma(\Delta\Delta C_{ant})$) is 1-2 mol m^{-2} dec^{-1}, while the ensemble mean decadal change ($\Delta\Delta C_{ant}$) is 2-4 mol m^{-2} dec^{-1} (figure 1). In the subtropical North Atlantic, $\sigma(\Delta\Delta C_{ant})$ is ~1 mol m^{-2} dec^{-1}, while the externally forced $\Delta\Delta C_{ant}$ is 2-3 mol m^{-2} dec^{-1}. The Arctic is characterized by elevated internal variability and high externally forced changes in the decadal C_{ant} storage changes (figure 1). Internal variability also plays a key role in decadal storage changes in regions that do not show large externally forced decadal changes, such as the subtropical North Pacific and the southern Indian Ocean (figure 1). As such, our analysis indicates that internal variability and external forcing both play key roles in regional, decadal ocean C_{ant} storage changes.

The impact of regional internal variability on decadal C_{ant} storage changes varies with depth (figure 2(b)). In the surface ocean, $\sigma(\Delta\Delta C_{ant})$ is largest in the tropical Pacific, with $\sigma(\Delta\Delta C_{ant})$ becoming more pronounced in the eastern Tropical Pacific at 100 m depth (figure 2(b)). The most pronounced internal variability in decadal C_{ant} storage changes in the upper ocean occurs at a depth of 300 m, where $\sigma(\Delta\Delta C_{ant})$ exceeds 4 mmol m^{-3} dec^{-1} in the western tropical Pacific, subpolar North Pacific, subpolar North Atlantic, subtropical South Indian, and in all basin sectors of the Southern Ocean (figure 2(b)). At 500 m, the highest $\sigma(\Delta\Delta C_{ant})$ values occur in the subtropical South Indian, subpolar North Atlantic, and Arctic Ocean (figure 2(b)). The zonal mean $\sigma(\Delta\Delta C_{ant})$ suggests that internal variability has the largest influence on decadal changes in C_{ant} within the thermocline of all ocean basins (figure 3, lower panel).

Regions characterized by high internal variability in decadal C_{ant} storage changes tend to align with the edges of the subtropical gyres. This is best illustrated in figures 1(b) and 2(b), where the colors indicate $\sigma(\Delta\Delta C_{ant})$, and the contours indicate the modeled BSF. The highest $\sigma(\Delta\Delta C_{ant})$ values coincide with closely spaced streamfunction contours, both for the column inventory (figure 1(b)) and the depth-resolved $\sigma(\Delta\Delta C_{ant})$ (figure 2(b)). The correspondence between $\sigma(\Delta\Delta C_{ant})$ and the streamfunction is most pronounced at 300 m, where CESM2-LE shows pronounced internal variability in decadal ocean C_{ant} storage changes at the northern and southern edges of the North Pacific and North Atlantic subtropical gyres, the northern edge of the South Pacific subtropical gyre, and the northern edge of the Indian Ocean subtropical gyre (figure 2(b)). Additionally, figure 3 lower panel highlights that all basins show internal variability as the driver of oceanic C_{ant} storage along the 'shoulders' of the subtropical gyres, with highest variability (2–4 mmol m^{-3} dec^{-1}) seen between 250 to 500 m depth.

Internal variability in upper ocean (0–3000 m) integrated C_{ant} has high spectral power on 3–7 yr, 7–20 yr, and 20+ year frequencies (figures 4 and S4). Tropical Pacific C_{ant} is characterized by large internal variance on 3–7 yr frequencies, as is C_{ant} in the Southern Ocean, northern Pacific, and southern Indian, Pacific, and South Atlantic. Though not as pronounced, the internal variance in C_{ant} in the extratropics has high spectral power at 7–20 and 20+ year frequencies. Low-frequency (20+ year) internal variability in Atlantic and Southern Ocean C_{ant} gradually increases in power from the surface to ~500 m (figure S4). Thus, results from our spectral analysis demonstrate that the dominant timescales of C_{ant} internal variability in the extratropics is 7–20+ years, which is the approximate repetition of the hydrographic surveys used to determine the decadal and multi-decadal changes in the ocean C_{ant} inventory.

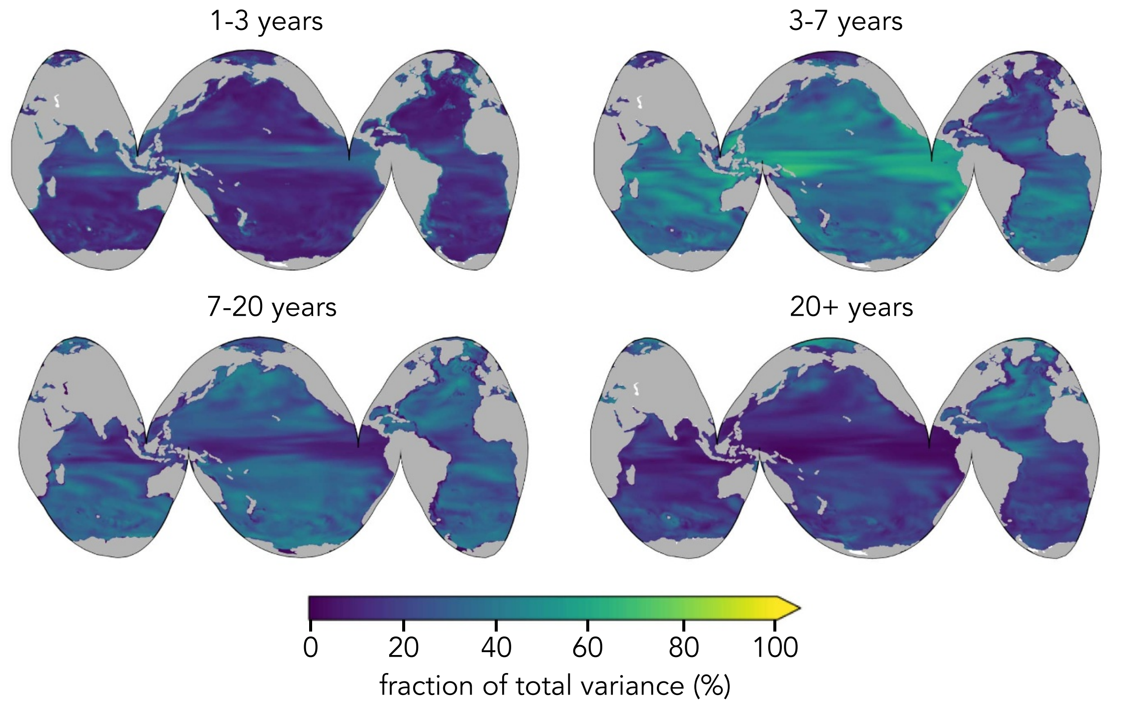

Figure 4. The fractional variance (%) of the spectral power in 1–3, 3–7, 7–20, and 20+ year bands of C_{ant} internal variability in the upper ocean (top 3000 (m), calculated from 1988 to 2014 using all CESM2-LE members.

4. Conclusions and discussion

This study uses CESM2-LE to investigate the influence of external forcing and internal climate variability on historical changes in interior ocean C_{ant} over 1994–2014. The externally forced, decadal changes in C_{ant} storage are positive nearly everywhere, with storage rates increasing fastest in the North Atlantic, Arctic, and subtropical South Atlantic at 300–500 m from the first decade to the second. Internal climate variability imprints on the decadal changes in C_{ant} storage, and on regional scales, is the same order of magnitude as the externally forced, decadal changes. We find large magnitude internal variability in C_{ant} decadal changes at 300 m and at the edges of the subtropical gyres in all basins. Internal variance in the extratropical storage of C_{ant} has substantial spectral power on 7–20+ year timescales. We conclude that the approximately decadal repetitions of hydrographic surveys may produce C_{ant} decadal storage change estimates that are heavily influenced by internal climate variability.

We find that both the externally forced change and internal climate variability play key roles in the decadal changes in oceanic C_{ant} storage over the top 3000 m. The observation-based study of Müller *et al* (2023) reports decreasing rates of C_{ant} storage over the top 3000 m in the North Atlantic and the Pacific and Indian sectors of the Southern Ocean, and increasing rates of C_{ant} storage on the southern edge of the subtropical gyre in the South Atlantic. The observed decadal storage changes in Müller *et al* (2023) are believed to be a combination of externally forced and internally derived changes (described as ‘steady state’ and ‘non-steady state’, respectively, in Müller *et al* (2023); further discussed in Olsen *et al* (2024)). Real-world observations are akin to a single ensemble member, and CESM2-LE can produce a range of decadal changes in C_{ant} that are both similar to, and starkly different from the changes estimated using real world observations (see, e.g. figure S3). Using the ensemble mean of 100 different possible scenarios, our study establishes that the externally forced, decadal changes in C_{ant} storage are positive almost everywhere. Thus, the modeled response to external forcing, such as increasing atmospheric CO_2 and any subsequent, externally forced changes in ocean circulation (such as a weakening of the AMOC and a reduction in the ocean’s buffer capacity, as suggested in Müller *et al* 2023), act to increase C_{ant} storage nearly everywhere from one decade to the next. Given that changes due to external forcing are positive almost everywhere, the observed negative decadal storage changes reported in Müller *et al* (2023) are likely driven by internal variability.

Internal climate variability has the largest influence on decadal changes in C_{ant} storage on the edges of the subtropical gyres. Recent studies document substantial interannual variability in the extent of the subtropical gyres in the Pacific and Atlantic basins (Kavanaugh *et al* 2018, Drouin *et al* 2021), which may be linked to modes of internal climate variability (Kavanaugh *et al* 2018) and produce variability in biogeochemical tracers (McClain *et al* 2004). Our study adds to this literature by demonstrating that subtropical gyre boundary variability imprints on the decadal trends in ocean C_{ant} storage. The western boundary currents that define the poleward extent of the subtropical gyres (e.g. Gulf Stream, Kuroshio Current) are characterized by turbulent mesoscale eddy processes that are highly variable; our research suggests large ensemble standard deviation in C_{ant} storage changes in these regions.

Internal variability in upper ocean C_{ant} inventory (figure 4) shows high spectral power on 3–7 year, 7–20 year, and 20+ year frequencies, indicating that ENSO (Feely *et al* 1999, 2006), PDO (Zhang *et al* 1997), AMOC (Buckley and Marshall 2016, Zhang *et al* 2019), and other low-frequency oscillatory climate modes drive internal variability in C_{ant}. Thus, our study suggests that the approximately decadal repetitions of hydrographic surveys may produce C_{ant} storage change estimates that are heavily influenced by internal climate variability. Additional observational studies, to include enhanced surveying in certain regions (for example, the equatorial Pacific every second year), are needed to better understand the drivers of C_{ant} storage changes in the real world. Interpretation of real-world changes would also benefit from understanding the phasing of internal climate variability and its influence on oceanic C_{ant} inventory.

Our findings are accompanied by several caveats. Like other Earth system models, CESM2-LE underestimates the ocean C_{ant} inventory's increase with time as compared to observations (figure S1; Mikaloff Fletcher *et al* 2006, DeVries *et al* 2019). As such, the externally forced changes in C_{ant} storage that we document here are likely smaller than those that have occurred in the real world. Further, we document high C_{ant} internal variability in eddy-rich regions, but the CESM2-LE experiment was conducted using a nominal 1° ocean model grid with parameterized subgrid-scale processes such as eddies. Reassuringly, decadal changes in C_{ant} storage estimated from a high-resolution (0.1°) ocean-ice hindcast simulation of CESM2 indicate high spatial variability at the edges of the subtropical gyres (figure S2; Krumhardt *et al* 2024), an indication of the large influence of internal variability on the decadal trends in these regions.

Internal climate variability modulates the decadal changes in C_{ant} storage, impacting some regions more than others, and, in some cases, changes due to internal variability are as large as the externally forced change. This study extends on previous literature that analyzes changes in the oceanic C_{ant} inventory (Sabine *et al* 2004, Mikaloff Fletcher *et al* 2006, Gruber *et al* 2009, 2019a, Khatiwala *et al* 2009, Wanninkhof *et al* 2010, Müller *et al* 2023, Olivarez *et al* 2024) by using a Large Ensemble to demonstrate that the changing inventory of C_{ant} on decadal timescales is influenced by both external forcing and internal climate variability. We quantify where and how much internal climate variability influences decadal C_{ant} storage changes, which will improve our ability to accurately project future changes in the ocean carbon reservoir.

Data availability statement

No new data were created or analysed in this study.

Acknowledgments

We would like to acknowledge high-performance computing support from Derecho (Computational and Information Systems Laboratory 2019) provided by NSF NCAR's Computational and Information Systems Laboratory, sponsored by the National Science Foundation. We are grateful for support from the National Science Foundation (OCE-1752724, OCE-1948664, and the Graduate Research Fellowship Program). This work benefited from computational assistance from R X Brady, S Mogen, and J Coupe; and from discussions with N Gruber and P Landschützer. We acknowledge previous work done by the CESM Large Ensemble Community Project.

The CESM2-LE source code is freely available from NCAR's Community Earth System Model version 2 (CESM2) (Danabasoglu *et al* 2020).

ORCID iDs

Holly C Olivarez https://orcid.org/0000-0002-8994-7967
Nicole S Lovenduski https://orcid.org/0000-0001-5893-1009
Elizabeth Maroon https://orcid.org/0000-0002-1660-7822
Jens D Müller https://orcid.org/0000-0003-3137-0883
Amanda R Fay https://orcid.org/0000-0003-3534-1932
Kristen M Krumhardt https://orcid.org/0000-0002-8980-056X
Michael N Levy https://orcid.org/0000-0001-6553-2153
Keith Lindsay https://orcid.org/0000-0002-3672-1665
Galen A McKinley https://orcid.org/0000-0002-4072-9221
Jamin K Rader https://orcid.org/0000-0002-2204-5977

References

Buckley M W and Marshall J 2016 Observations, inferences and mechanisms of the Atlantic Meridional Overturning Circulation: a review *Rev. Geophys.* **54** 5–63

Canadell J G *et al* 2021 Global carbon and other biogeochemical cycles and feedbacks *Climate Change 2021: The Physical Science Basis. Contribution of Working Group I to the Sixth Assessment Report of the Intergovernmental Panel on Climate Change*, ed V Masson-Delmotte

Computational, and Information Systems Laboratory 2019 Cheyenne: HPE/SGI ICE XA System (Climate Simulation Laboratory Boulder, CO: U.S. National Science Foundation National Center for Atmospheric Research)

Danabasoglu G, Bates S C, Briegleb B P, Jayne S R, Jochum M, Large W G, Peacock S and Yeager S G 2012 The CCSM4 Ocean Component *J. Clim.* **25** 1361–89

Danabasoglu G *et al* 2020 The community earth system model version 2 (CESM2) *J. Adv. Model. Earth Syst.* **12** 916

DeRepentigny P *et al* 2022 Enhanced simulated early 21st century Arctic sea ice loss due to CMIP6 biomass burning emissions *Sci. Adv.* **8** eabo2405

DeVries T *et al* 2019 Decadal trends in the ocean carbon sink *Proc. Natl Acad. Sci.* **116** 11646–51

Drouin K L, Lozier M S and Johns W E 2021 Variability and trends of the south atlantic subtropical gyre *J. Geophys. Res.* **126** 2020JC016405

Fay A R, McKinley G A, Lovenduski N S, Eddebbar Y, Levy M N, Long M C, Olivarez H C and Rustagi R R 2023 Immediate and long-lasting impacts of the Mt. Pinatubo eruption on ocean oxygen and carbon inventories *Glob. Biogeochem. Cycles* **37** 2022GB007513

Feely R A, Wanninkhof R, Takahashi T and Tans P 1999 Influence of El Niño on the equatorial Pacific contribution to atmospheric CO_2 accumulation *Nature* **398** 597–601

Feely R A, Takahashi T, Wanninkhof R, McPhaden M J, Cosca C E, Sutherland S C and Carr M-E 2006 Decadal variability of the air-sea CO_2 fluxes in the equatorial Pacific Ocean *J. Geophys. Res.: Oceans* **111** 129

Graven H D, Gruber N, Key R, Khatiwala S and Giraud X 2012 Changing controls on oceanic radiocarbon: New insights on shallow-to-deep ocean exchange and anthropogenic CO_2 uptake *J. Geophys. Res.: Oceans* **117** 74

Gruber N, Landschützer P and Lovenduski N S 2019a The variable southern ocean carbon sink *Ann. Rev. Mar. Sci.* **11** 159–86

Gruber N *et al* 2009 Oceanic sources, sinks and transport of atmospheric CO_2 *Glob. Biogeochem. Cycles* **23** GB1005

Gruber N *et al* 2019b The Oceanic Sink for Anthropogenic CO_2 from 1994 to 2007 *Science* **363** 1193

Hauck J *et al* 2020 Consistency and challenges in the ocean carbon sink estimate for the Global Carbon Budget *Front. Mar. Sci.* **7** 852

Heideman M T, Johnson D H and Burrus C S 1985 Gauss and the history of the fast fourier transform *Arch. Hist. Exact Sci.* **34** 265–77

Kavanaugh M T, Church M J, Davis C O, Karl D M, Letelier R M and Doney S C 2018 ALOHA from the edge: reconciling three decades of in situ Eulerian observations and geographic variability in the North Pacific Subtropical Gyre *Front. Mar. Sci.* **5** 130

Khatiwala S, Primeau F and Hall T 2009 Reconstruction of the history of anthropogenic CO_2 concentrations in the ocean *Nature* **462** 346–9

Khatiwala S *et al* 2013 Global ocean storage of anthropogenic carbon *Biogeosciences* **10** 2169–91

Kobayashi S *et al* 2015 The JRA-55 reanalysis: general specifications and basic characteristics *J. Meteor. Soc. Japan* **93** 5–48

Krumhardt K M *et al* 2024 From nutrients to fish: impacts of mesoscale processes in a global CESM-FEISTY eddying ocean model framework *Prog. Oceanogr.* **227** 103,314

Landschützer P, Ilyina T and Lovenduski N S 2019 Detecting regional modes of variability in observation-based surface ocean pCO_2 *Geophys. Res. Lett.* **46** 2670–9

Long M C *et al* 2021 Simulations with the Marine Biogeochemistry Library (MARBL *J. Adv. Modeling Earth Syst.* **13** e2021MS002

Lovenduski N S, Gruber N, Doney S C and Lima I D 2007 Enhanced CO_2 outgassing in the Southern Ocean from a positive phase of the Southern Annular Mode *Glob. Biogeochem. Cycles* **21** GB2026

Lovenduski N S, Gruber N and Doney S C 2008 Toward a mechanistic understanding of the decadal trends in the Southern Ocean carbon sink *Glob. Biogeochem. Cycles* **22** GB3016

Mantua N J, Hare S R, Zhang Y, Wallace J M and Francis R C 1997 A pacific interdecadal climate oscillation with impacts on salmon production *Bull. Am. Meteorol. Soc.* **78** 1069–80

McClain C R, Signorini S R and Christian J R 2004 Subtropical gyre variability observed by ocean-color satellites *Deep Sea Res.* II **51** 281–301

McKinley G A, Fay A R, Lovenduski N S and Pilcher D J 2017 Natural variability and anthropogenic trends in the ocean carbon sink *Annu. Rev. Mar. Sci.* **9** 125–50

McKinley G A, Fay A R, Eddebbar Y A, Gloege L and Lovenduski N S 2020 External forcing explains recent decadal variability of the ocean carbon sink *AGU Adv.* **1** e2019AV000

Meinshausen M *et al* 2017 Historical greenhouse gas concentrations for climate modelling (CMIP6) *Geosci. Model Dev.* **10** 2057–116

Mikaloff Fletcher S E *et al* 2006 Inverse estimates of anthropogenic CO_2 uptake, transport and storage by the ocean *Glob. Biogeochem. Cycles* **20** 30

Moore J K and Braucher O 2008 Sedimentary and mineral dust sources of dissolved iron to the world ocean *Biogeosciences* **5** 631–56

Moore J K, Doney S C and Lindsay K 2004 Upper ocean ecosystem dynamics and iron cycling in a global three-dimensional model *Glob. Biogeochem. Cycles* **18** 20

Moore J K, Lindsay K, Doney S C, Long M C and Misumi K 2013 Marine ecosystem dynamics and biogeochemical cycling in the Community Earth System Model [CESM1(BGC)]: comparison of the 1990s with the 2090s under the RCP4.5 and RCP8.5 scenarios *J. Clim.* **26** 9291–312

Müller J D *et al* 2023 Decadal trends in the oceanic storage of anthropogenic carbon from 1994 to 2014 *AGU Adv.* **4** 875

Oka E, Qiu B, Takatani Y, Enyo K, Sasano D, Kosugi N, Ishii M, Nakano T and Suga T 2015 Decadal variability of subtropical mode water subduction and its impact on biogeochemistry *J. Oceanogr.* **71** 389–400

Olivarez H C, Lovenduski N S, Eddebbar Y A, Fay A R, McKinley G A, Levy M N and Long M C 2024 How does the pinatubo eruption influence our understanding of long-term changes in ocean biogeochemistry? *Geophys. Res. Lett.* **51** 431

Olsen A, Rajasakaren B, Jeansson E, Lauvset S K, Omar A M and Becker M 2024 In the wake of deeper convection: nonsteady state anthropogenic carbon in the greenland sea *J. Geophys. Res. Oceans* **129** 462

Revelle R and Suess H E 1957 Carbon dioxide exchange between atmosphere and ocean and the question of an increase of atmospheric CO_2 during the past decades *Tellus* **9** 18–27

Rodgers K B *et al* 2021 Ubiquity of human-induced changes in climate variability *Earth Syst. Dyn.* **12** 1393–411

Sabine C L *et al* 2004 The Oceanic Sink for Anthropogenic CO_2 *Science* **305** 367–71

Sarmiento J L, Orr J C and Siegenthaler U 1992 A perturbation simulation of CO_2 uptake in an ocean general circulation model *J. Geophys. Res.* **97** 3621–45

Smith R et al 2010 The parallel ocean program (POP) reference manual, *Technical Report* LAUR-10-01853 Los Alamos National Laboratory, Los Alamos, NM

Terhaar J, Frölicher T L and Joos F 2022 Observation-constrained estimates of the global ocean carbon sink from Earth system models *Biogeosciences* **19** 4431–57

Terhaar J, Goris N, Müller J D, DeVries T, Gruber N, Hauck J, Perez F F and Séférian R 2024 Assessment of global ocean biogeochemistry models for ocean carbon sink estimates in RECCAP2 and recommendations for future studies *J. Adv. Modeling Earth Syst.* **16** e2023MS003

Tsujino H *et al* 2020 Evaluation of global ocean–sea-ice model simulations based on the experimental protocols of the Ocean Model Intercomparison Project phase 2 (OMIP-2 *Geosci. Model Dev.* **13** 3643–708

Wanninkhof R, Doney S C, Bullister J L, Levine N M, Warner M and Gruber N 2010 Detecting anthropogenic CO_2 changes in the interior Atlantic Ocean between 1989 and 2005 *J. Geophys. Res.* **115** 251

Zhang R, Sutton R, Danabasoglu G, Kwon Y-O, Marsh R, Yeager S G, Amrhein D E and Little C M 2019 A review of the role of the atlantic meridional overturning circulation in Atlantic Multidecadal variability and associated climate impacts *Rev. Geophys.* **57** 316–75

Zhang Y, Wallace J M and Battisti D S 1997 ENSO-like Interdecadal Variability: 1900–93 *J. Clim.* **10** 1004–20